Aerosol and Air Quality Research, 12: 951–960, 2012
Copyright © Taiwan Association for Aerosol Research
ISSN: 1680-8584 print / 2071-1409 online
doi: 10.4209/aaqr.2012.01.0011

Size Differentiation of Individual Atmospheric Aerosol during Winter in Xi'an, China

Tafeng Hu[1*], Junji Cao[1,4*], Zhenxing Shen[2], Gehui Wang[1,4], Shuncheng Lee[3], Kinfai Ho[1,3]

[1] *Key Laboratory of Aerosol, SKLLQG, Institute of Earth Environment, Chinese Academy of Sciences, Xi'an 710075, China*
[2] *Department of Environmental Science and Engineering, Xi'an Jiaotong University, Xi'an 710049, China*
[3] *Department of Civil and Structural Engineering, The Hong Kong Polytechnic University, Hong Kong, China*
[4] *Institute of Global Environmental Change, Xi'an Jiaotong University, Xi'an 710049, China*

ABSTRACT

Airborne particulate matter (including TSP, PM_{10}, $PM_{2.5}$, and PM_1) were collected at an urban site in Xi'an during winter 2010. Individual particles were analyzed using scanning electron microscopy and energy dispersive X-ray spectrometer (SEM-EDX). The morphologies, size distributions, and relative abundance of aerosol particles in each size were summarized. The monomodal particle size distribution was found in all the samples under different weather conditions, with the peaks located at less than 1.0 µm. The majority of particles were composed of soot, mineral dust, and tar balls, with minor fly ash particles. Soot aggregates were the predominant species (in numbers), ranging from 56.6% in TSP on a sunny day to 86.3% in PM_1 on a cloudy day, with an average of 73.2% in all the samples. The particle mass concentration and chemical composition, including water-soluble inorganic ions, elemental compositions, organic carbon (OC) and elemental carbon (EC) contents of 24-hr integrated $PM_{2.5}$, were also subject to chemical bulk analysis. Soot was predominantly observed in the $PM_{2.5}$ samples (from 74.7% to 82.7% in numbers), whereas EC accounted for only a small amount (< 8%) of the $PM_{2.5}$ mass. Corresponding to the mass concentrations of geological materials (29.2%, 44.5%, and 37.3% on sunny, cloudy, and hazy days), the number concentrations of mineral dust and fly ash particles on the sunny, cloudy, and hazy days were 14.6%, 7.1%, and 7.7%, respectively.

Keywords: Size-differentiated aerosols; Chemical composition; Scanning electron microscopy.

INTRODUCTION

The physico-chemical properties of airborne particulate matter (PM) are of concern primarily due to its adverse human health effects and influence on climate change through its contribution to radiative forcing. The particle size and chemical composition of the atmospheric aerosol are the main factors that determine the particles' effects on atmospheric visibility (Watson, 2002). Aerosol chemical composition is also a strong indicator of particle sources (Watson *et al.*, 2001; Harrison *et al.*, 2004). With reference to human health effects, epidemiological studies have shown an association between particle chemical composition and hospital admission (Harrison and Yin, 2000; Laden *et al.*, 2000; Yin and Harrison, 2008). There is also convincing evidence that particle size distribution determines the position of deposition in the human lung and has a major influence upon toxicity (Anderson *et al.*, 2001). Therefore, legislation in the United States has progressively moved the emphasis of air-quality regulation from TSP (total suspended particles) to PM_{10} and to $PM_{2.5}$ (US EPA, 2004; Edgerton *et al.*, 2009).

Xi'an, the largest city in Northwest China, is the capital of Shaanxi province at the south edge of the Loess Plateau (400 m above sea level at 33°29′–34°44′N, 107°40′–109°49′E). The climate of Xi'an is dominated by the East Asian monsoon. The population of Xi'an has grown from more than 7.4 million in 2000 to more than 8.4 million in 2010. Although nature gas has partly replaced coal for heating in downtown Xi'an, the number of motor vehicles inside this city has increased from approximately half a million in 2006 to more than 1.3 million in 2010. Due to a rapid increase of vehicles and the growth in energy consumption over the past few decades, Xi'an is facing serious air quality problems, mainly due to the high aerosol loadings in the region (Zhang *et al.*, 2002; Cao *et al.*, 2005a; Shen *et al.*, 2008; Cao *et al.*, 2009). Haze days, defined as the atmospheric visibility is less than 10 km by China Meteorological Agency, has been frequently observed in Xi'an and is closely related to local pollution and meteorological conditions (Shen *et al.*, 2009). The chemical

---

[*] Corresponding author. Tel.: 86-29-8832-6128;
Fax: 86-29-8832-0456
E-mail address: hutf@ieecas.cn; cao@loess.llqg.ac.cn

composition and sources of TSP, PM with aerodynamic diameters ≤ 10 µm (PM_{10}), ≤ 2.5 µm ($PM_{2.5}$), and ≤ 1 µm (PM_1) have been measured in several recent studies by means of chemical bulk analysis methods (Cao *et al.*, 2005b; Shen *et al.*, 2008; 2009; 2011), including Energy Dispersive X-Ray Fluorescence (ED-XRF), Ion Chromatography (IC), and Carbon Analyzer. Detailed information on mass, trace elements, carbonaceous aerosol, and secondary aerosol concentrations during dust storm and air pollution episodes has been obtained in those studies. In recent years several worldwide studies on aerosol particle number concentrations and mass size distribution have been published (Cheng and Lin, 2010; Avino *et al.*, 2011; Diapouli *et al.*, 2011; Hussein *et al.*, 2011). However, little is known about the physico-chemical properties of individual particulate matters over Xi'an.

The study pursued two objectives. First, size distribution, morphology, and elemental composition of approximately 9,500 individual particles in TSP, PM_{10}, $PM_{2.5}$, and PM_1 samples were analyzed using SEM-EDX to examine their sources on three winter days with distinct meteorological conditions. Furthermore, the variation between major constituents in $PM_{2.5}$ characterized by number concentrations according to individual particle analysis and by mass concentrations according to bulk analysis methods was intercompared.

METHODOLOGY

Sample Collection

Airborne particle samples were collected on the roof of the office building in the Institute of Earth Environment, Chinese Academy of Sciences (about 10 m above ground level) on three separate days during winter (9, 10, and 13 December 2010). The sampling site located about 15 km south of downtown Xi'an and was surrounded by residential areas and office buildings (Fig.1).

The sampling campaigns were carried out for TSP, PM_{10}, $PM_{2.5}$, and PM_1 simultaneously in order to obtain a comparative result of the measurement. Samples for individual particle analysis were collected onto 47 mm polycarbonate Nuclepore filters (0.4 µm in porosity; Whatman International Ltd., Maidstone, UK) using three mini-vol air samplers (for TSP, PM_{10}, and $PM_{2.5}$, Airmetrics Corp., Springfield, OR, USA), and one BGI frmOMNI Ambient Air Sampler (for PM_1, BGI Inc, Waltham, MA, USA). Under pre-optimized 2-hour sampling duration, particles were collected in a single layer onto the filters with minimal particle-to-particle contact. An additional mini-vol air sampler was deployed to collect 24-hour integrated $PM_{2.5}$ samples onto quartz filters (Whatman QM/A, Maidstone, UK) for bulk chemical analyses. The operating flow rate of all samplers was 5 L/min. The sampling information was detailed in Table 1. Meteorological conditions during the sampling period were recorded by the Shaanxi Meteorological Bureau. After sampling, filters were placed in plastic cassettes and stored in a refrigerator at 4°C until analyzed.

Sample Analyses

Small rectangular sections (approximately 10 × 10 mm) were cut from the polycarbonate filters and mounted on the SEM stubs with conductive adhesive carbon tape. Samples were coated under vacuum with gold and analyzed using a computer-controlled JEOL JSM-6460 LV SEM (Japan Electron Optics Laboratory Co. Ltd., JP) under 20 kV accelerating voltage at a work distance of 10 mm. For each sample, ten secondary electron images (SEI) were acquired with magnifications from 1000 × to 5000 ×, depending on the particle size in respective image views. The diameter of each individual particle was measured from SEI images by IMAGE PRO PLUS 5.0 software (Media Cybernetics, Inc., Silver Spring, MD, USA), and was estimated as the average of the longest dimension and its orthogonal width. All particles with a diameter larger than 0.4 µm in each image were measured to obtain size distributions. Individual particles larger than 0.4 µm in each sample were selected for elemental analyses manually using NORAN SYSTEM

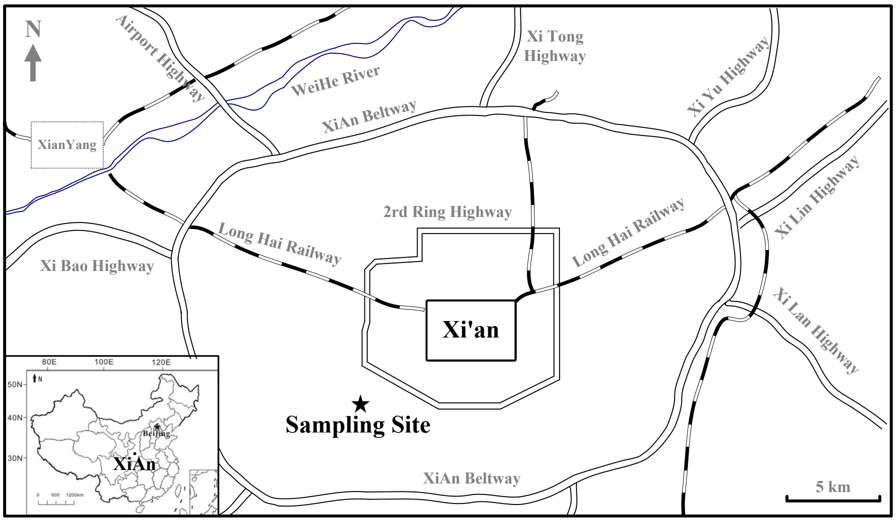

Fig. 1. Location of sampling site in Xi'an city are Marked with Stars.

Table 1. Sampling information with the weather condition, averaged temperature (T) and relative humidity (RH), prevailing wind direction (WD), wind speed (WS), and gas concentrations monitored at the urban site during sampling periods for SEM/EDX analysis.

Date	Start Time UTC	2-hour Sampling (Polycarbonate Filter)	24-hour Sampling (Quartz Filter)	Weather	T (°C)	RH (%)	WD	WS (m/s)	Visibility (km)
09 Dec. 2010	02:00	TSP,PM_{10},$PM_{2.5}$,PM_1	$PM_{2.5}$	Sunny	8.5	34	W	1.1	18
10 Dec. 2010	02:00	TSP,PM_{10},$PM_{2.5}$,PM_1	$PM_{2.5}$	Cloudy	5.7	43	NW	1.0	12
13 Dec. 2010	02:00	TSP,PM_{10},$PM_{2.5}$,PM_1	$PM_{2.5}$	Haze	4.8	51	NE	0.9	4

SIX Si-Li EDX detector with an ultra thin window (Thermo Electron Corporation, Waltham, MA, USA). The EDX counting time was 30 s live-time for each particle at magnifications of 1000 ×, 3000 ×, 5000 ×, and 10000 ×, according to particle size in respective images. X-ray peak intensities for each element were converted into weight fractions using the EDX software without ZAF correction (Hu *et al.*, 2009).

Quartz filters were analyzed gravimetrically for $PM_{2.5}$ mass concentrations by a Sartorius MC5 electronic microbalance with a ± 1 µg sensitivity (Sartorius, Göttingen, Germany) after 24-hour equilibration at temperature between 20 and 23°C and RH between 35 and 45%.

A punch of 0.5 cm^2 from each quartz filter was analyzed for organic carbon (OC) and elemental carbon (EC) by the IMPROVE A thermal/optical protocol using a DRI Model 2001 thermal/optical carbon analyzer (Atmoslytic Inc., Calabasas, CA, USA). Quality assurance/quality control (QA/QC) procedures were described by Cao *et al.* (2003).

One-fourth of each quartz filter sample was used for gravimetric determinations of aerosol ion mass concentrations. Three anions (Cl^-, NO_3^- and SO_4^{2-}) and five cations (Na^+, NH_4^+, K^+, Mg^{2+} and Ca^{2+}) were measured by a Dionex-600 Ion Chromatograph (Dionex Inc., Sunnyvale, CA, USA). A CS12 column (150 × 4 mm) and an AS14 column (150 × 4 mm) were used for cation and anion analysis, respectively. Field blank levels were averaged, subtracted, and standard deviations were propagated to the measurement precisions (Chow and Watson, 1999). Minimum detection limits (MDLs) were 15 µg/L for Na^+, NH_4^+, K^+, Mg^{2+}, Ca^{2+}, and NO_3^-; 0.5 µg/L for Cl^-; and 20 µg/L for SO_4^{2-}. Ten percent of the samples were submitted for replicate analyses.

Concentrations of 13 elements (K, Ca, Ti, Cr, Mn, Fe, Ni, Zn, As, Br, Mo, Cd, and Pb) collected on the $PM_{2.5}$ quartz-fibre filters were determined using an Epsilon 5 ED-XRF (PANalytical B. V., the Netherlands). The X-ray source is a side-window X-ray tube with a gadolinium anode, and it is operated at an accelerating voltage of 25 to 100 kV and a current of 0.5 to 24 mA (maximum power: 600 W). Each sample was analyzed for 30 mins. A spectrum of X-ray counts versus photon energy was acquired during analysis, with the individual peak energies matching to specific elements, and peak areas corresponding to elemental concentrations (Xu *et al.*, 2011).

RESULTS AND DISCUSSION

Particle Size Distribution

The number–size distributions of individual particles on each size filters were shown in Fig. 2. The meteorological conditions, including averaged temperature, relative humidity, and dominant wind direction varied from day to day on the three sampling days. However, the averaged wind speeds were similar and remained at a relative low level during the sampling period. Thus, a monomodal particle size distribution was found in all the samples with the peaks located less than 1.0 µm. Previous study has suggested a statistical association between health effects and the particle composition in submicron fraction (Huang *et al.* 2003) presumably due to the fact that fine particles can penetrate into the alveolar region of the lungs. Moreover, most particles (by mass) in the submicron size range arise from anthropogenic sources. Despite the variability of samplers, the measured particles were mainly < 1.0 µm in size, implying that the abundance of fine particles within each size range under different weather conditions should be controllable by regulatory action.

Particle Morphology

The particles were grouped into five dominant types according to their morphologies and elemental compositions as soot aggregate, tar ball, mineral dust, salt particles and fly ash. The typical morphologies of individual particles collected on polycarbonate filters were shown in Fig. 3.

Carbonaceous particles with dominant C and O peaks in their spectra were designated as soot or tar ball particles according to their particulate morphologies. As for particle number, soot aggregates were the most frequently observed on each size range filters and was clearly distinguishable from other particle types due to its unique morphology. Mostly chain-like and cluster-like soot aggregates contained from less than ten to hundreds of spherules, each of which was 20 to 100 nm with diameter (Figs. 3(a) and (b)). Tar balls were mostly spheres with diameters less than or around 0.5 µm and were typically not agglomerated with other types of particles. Some of the tar balls were highly spherical particles with smooth surfaces, others were broken or shrunk hollow spheres (Figs. 3(c) and (d)). Tar balls are primarily associated with biomass burning or biofuel combustion, especially during smoldering burning conditions (Li *et al.*, 2003; Pósfai *et al.*, 2003; Chakrabarty *et al.*, 2006; Tivanski *et al.*, 2007). In previous studies, tar balls in African biomass smoke and in European polluted air were found with few particle diameters larger than 400 nm (Pósfai *et al.*, 2004; Hand *et al.*, 2005).

Identification of mineral dust, salt particles, and fly ash with dominant inorganic elements is based on their elemental

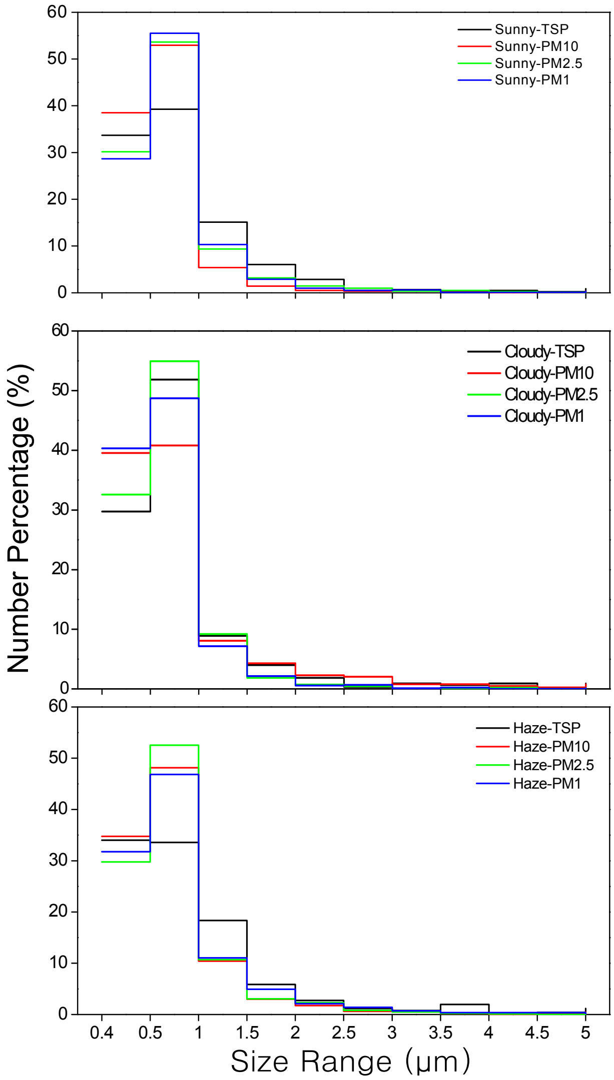

Fig. 2. Number percentages of particles in each size range of TSP, PM_{10}, $PM_{2.5}$, and PM_1 samples collected under different weather conditions.

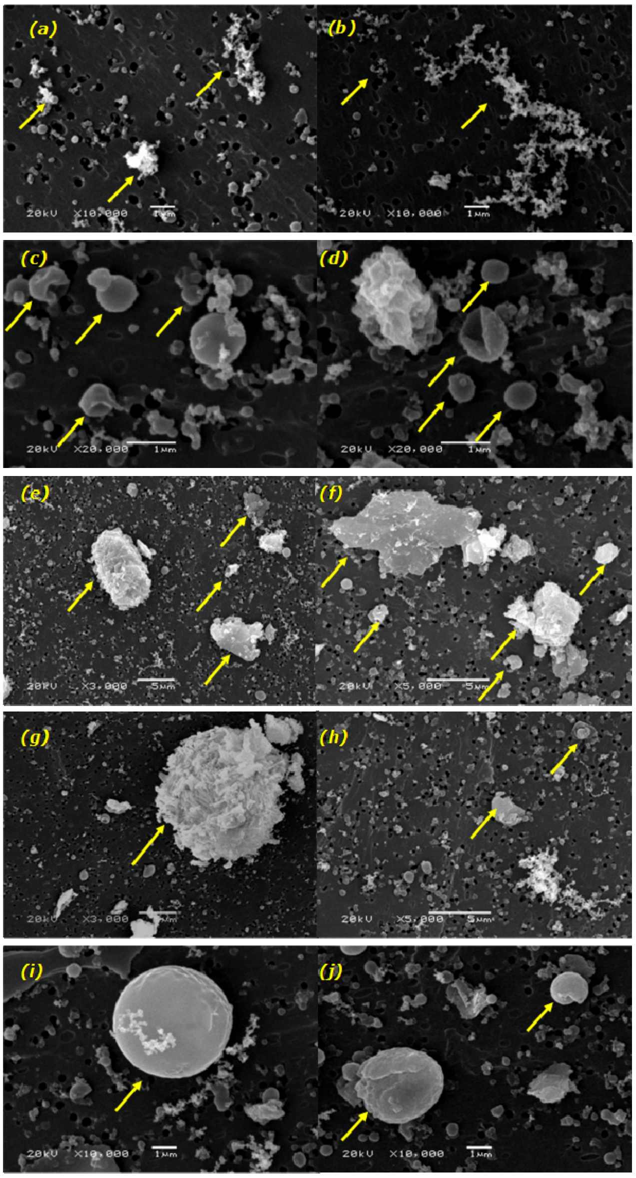

Fig. 3. The micrographs of typical individual particles loaded on polycarbonate filters: (a and b) soot aggregates; (c and d) tar balls; (e and f) mineral dusts; (g and h) salt particles; (i and j) fly ashes.

compositions by excluding C and O peaks from the spectra to avoid interference from the polycarbonate filter. Cl- and S-free particles with abundant Si, Al, and Fe were classified into mineral dust as quartz, aluminosilicate, silicate or Fe oxide (Figs. 3(e) and (f)). Fly ash particles were generally spherical or spherical aggregates adhering to other particles (Figs. 3(g) and (h)), and enriched by Al and Si, with relatively minor Na, Mg, Ca, Mn, and Fe. As evidences of particles from anthropogenic emissions (Zhang *et al.*, 2005, 2008), Cl-containing and/or S-containing particles without Si and Al were assigned to salt as chloride and/or sulphate (Figs. 3(i) and (j)).

Particle Type under Three Weather Conditions

The number percentages of each particle group were illustrated in Fig. 4. In previous study, the variability of $PM_{2.5}$ and its components was found closely related with meteorological variables, including temperature, relative humidity, precipitation, and circulation (Tai *et al.*, 2010). Besides, the differences in chemical composition of $PM_{2.5}$ and $PM_{1.0}$ were more dependent on typical components in fine fraction particles such as ammonium sulfate and ammonium nitrate than those residing primarily in the coarse fraction such as sea salt, calcium- and iron-rich dusts (Yin and Harrison, 2008). In this study, the correlations between number concentrations of major constituents and weather conditions or particle size ranges were weak, probably due to the limited amount of samples. As shown in Fig. 4, soot aggregate prevailed in all size range samples with an averaged number concentration of 73.2%, ranging from 56.6% in TSP on a sunny day to 86.3% in PM_1 on a cloudy day. Fine particles from combustion sources were considered to be the most dangerous to health (Laden *et al.*, 2000), higher number percentage of soot aggregate

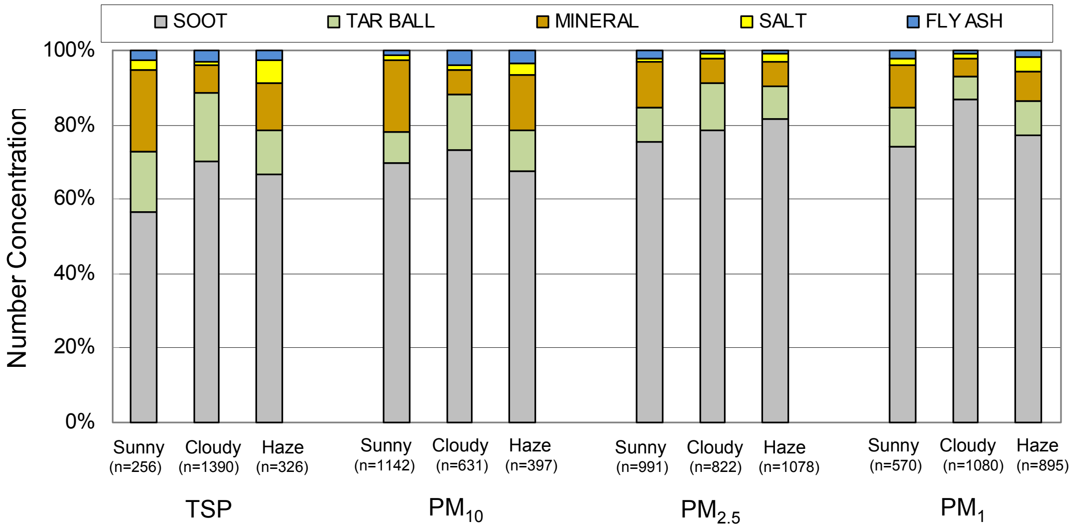

Fig. 4. Classification and particle number percentage of each group in different size range samples.

occurred in the Xi'an samples, implying a strong health risk. Due to their small density, soot particles are easily dispersed to areas far away from their sources and this extends their effects over large regions (Zhang *et al.*, 2001). The number percentages of tar ball (6.0–18.3%) in cloudy day samples were higher than those of mineral dust (5.0–7.5%), whereas in sunny day samples mineral dust occupied a higher range of 11.1–21.9% than tar ball (8.1–16.0%). Salt particles were much more abundant in haze day samples (2.1–6.1%) than in sunny day (0.6–2.7%) and cloudy day (1.1–1.5%) samples.

$PM_{2.5}$ Chemical Composition

The $PM_{2.5}$ mass concentrations on the sunny, cloudy, and haze days were 190.9, 213.1, 156.5 µg/m^3, respectively. All the three daily $PM_{2.5}$ concentrations exceed the U.S. National Ambient Air Quality Standards (NAAQS) 24-hour limit (35 µg/m^3). The highest concentration of the 13 elements under various weather conditions was chlorine, suggesting the heavy influence of anthropogenic sources, especially coal combustion and biomass burning for heating in winter. The OC and EC concentrations on the three sampling days were at the average level for winter $PM_{2.5}$ recorded in Xi'an city (Cao *et al.*, 2005a, 2009, 2011). The OC/EC ratios on the sunny, cloudy, and hazy sampling days were 2.5, 2.2, and 2.8, respectively, suggesting that coal combustion and vehicle emission plays an important role in carbonaceous aerosol's origins in Xi'an (Watson *et al.*, 2001; Cao *et al.*, 2005a; Shen *et al.*, 2010; Zhu *et al.*, 2010). The total $PM_{2.5}$ ion mass concentration on sunny day (51.5 µg/m^3) was slightly higher than those on cloudy (38.8 µg/m^3) and hazy (38.5 µg/m^3) sampling days, accounting to 26.9%, 18.2%, and 24.6% of total $PM_{2.5}$ mass, respectively. Cl^- concentration in the three samples were higher than the averaged concentrations in normal days (4.2 µg/m^3) obtained at another urban site in Xi'an (Shen *et al.*, 2009), but were still less abundant than those measured either in haze days (15.2 µg/m^3) or in straw combustion days (14.6 µg/m^3).

Comparison with Material Balance for $PM_{2.5}$

Material Balance for $PM_{2.5}$

The material balance approach has been used to estimate mass enclosure (Solomon *et al.*, 1989). Since ED-XRF does not analyze Al and Si, Fe is used to estimate the upper limit of geological material (Taylor and Mclennan, 1985). Previous studies have shown that Fe accounts for 4% of Asian dust and Chinese loess (Zhang *et al.*, 2002, 2003). Thus, the concentration of geological material was calculated by

$$C_{geological\ material} = (1/0.04) \times C_{Fe} \quad (1)$$

where C_{Fe} is the mass concentration of elemental Fe determined by ED-XRF.

The amount of organic material was determined by multiplying the amount of OC by 1.6 according to the study of Turpin and Lim (2001).

$$C_{organic\ material} = 1.6 \times OC \quad (2)$$

The material balances for geological material (crustal material), organic matter (OM), EC, ions (sum of Cl^-, NO_3^-, SO_4^{2-}, Na^+, NH_4^+, K^+, Mg^{2+}, and Ca^{2+}), and others (as the difference between the measured mass and the sum of the major components) for $PM_{2.5}$ under various winter weather conditions were shown in the lower box of Fig. 5. Besides, pie charts in the upper box of Fig. 5 illustrated the particle classification and number concentrations of major constituents in the same day $PM_{2.5}$ samples. The mass concentration results were based on the particle chemical composition determined by bulk analysis methods as XRF, IC, and Carbon Analyzer. The number concentration results were based on the particle morphologies and elemental compositions determined by individual analysis technique as SEM-EDX.

Carbonaceous Aerosol Particles

Obvious difference between mass and number

Table 2. Summary of 24-hr $PM_{2.5}$ chemical composition for samples acquired at a Xi'an urban site on three winter days with various weather conditions.

	Sunny day 09 Dec. 2010	Cloudy day 10 Dec. 2010	Hazy day 13 Dec. 2010
Mass	190.9	213.1	156.5
OC	37.0	35.4	23.5
EC	14.7	15.9	8.5
NO_3^-	14.0	10.3	10.0
SO_4^{2-}	12.5	11.1	11.6
Cl^-	11.3	9.0	7.2
NH_4^+	7.7	4.0	4.8
Mg^{2+}	0.1	0.2	0.0
Ca^{2+}	2.3	4.2	2.6
K^+	2.6	1.9	1.8
Na^+	0.7	0.8	0.1
K	3.0	3.4	2.5
Ca	3.5	7.3	4.0
Ti	231.9	385.5	200.0
Cr	31.0	16.4	8.8
Mn	150.7	247.1	184.3
Fe	2814.3	4724.0	2941.0
Ni	10.3	25.3	3.5
Zn	1849.6	6867.3	1574.0
As	44.3	29.8	29.8
Br	48.8	70.0	33.3
Mo	45.8	19.3	49.1
Cd	0.0	0.0	71.9
Pb	480.1	595.3	363.2

Unit: from mass to Ca, $\mu g/m^3$; from Ti to Pb, ng/m^3.

concentrations is shown in Fig. 5, generally predominant soot (in numbers) were observed in all samples, whereas EC occupied only a small amount (< 8%) of the $PM_{2.5}$ mass. In this study, soot refers to measurements with morphological detection by SEM-EDX and EC was analyzed on the basis of thermo-optical reflectance method by Carbon Analyzer. Generally, EC is emitted as loose chain- or cluster-like soot aggregates directly into the atmosphere from various combustion sources as fossil fuel, biofuel combustion and open biomass-burning fires (Bond *et al.*, 2004). Although EC was separated into two categories as char-EC and soot-EC (Watson *et al.*, 2005; Han *et al.*, 2007), char particles with characteristic morphological features similar to their source material were seldom observed in this study. Furthermore, soot particles could adsorb OC compounds when the combustion products cool down (Dachs and Eisenreich, 2000). Internally mixed soot aggregates with hygroscopic sulfate particles (Pósfai *et al.*, 1999) or nitric acid (Laskin *et al.*, 2005) have also been observed. In our individual particle analysis, mixed soot particles were included into "soot" group during classification process, whereas in our bulk analyses, their water-soluble part and organic coatings were determined as ions and OC mass, respectively. This variation between analytical methods may result in the underestimation of salt particle and organic tar ball number concentrations in Fig. 5.

In thermo-optical reflectance method, OC is operationally defined as the difference between TC and EC (OC = TC – EC). The division between OC and EC is dependent on the methods and analytical protocol selected. Since OC compounds contain majority of C and variable amounts of other elements, including O, H, and N, the original mass of organic materials is often estimated using conversion factors (e.g., 1.6 in this study). OM originates from various natural and anthropogenic activities, including particles from open biomass burning, fossil fuel combustion, residential wood combustion, refuse incineration, cooking, biological sources, organic soil dust, organic road dust components, chemical reactions (oxidation) and gas-to-particle conversion of volatile organic compounds (VOCs) in the atmosphere (Seinfeld and Pankow, 2003; Bond *et al.*, 2004; O'Dowd *et al.*, 2004; Sun and Ariya, 2006). In urban atmosphere the major OM sources came from fossil fuel and biofuel combustion (Bond *et al.*, 2004). Previous study found that biogenic particles (pollen, spore, and vegetative debris) were abundant in atmospheric $PM_{10–2.5}$ collected at two urban sites in summer and autumn (Edgerton *et al.*, 2009), but they were seldom observed in our winter study. Under our SEM-EDX observation, $PM_{2.5}$ samples contained spherical C-dominant particles. Those amorphous and heat-resistant particles have been named as "tar ball", a carbonaceous particle type distinct from soot (Pósfai *et al.*, 2003; 2004). Tar balls contain abundant OC and originate from biomass burning, especially during smouldering burning conditions (Pósfai *et al.*, 2003, 2004; Hand *et al.*, 2005; Chakrabarty *et al.*, 2006). Since soot aggregates coated with organic materials were assigned

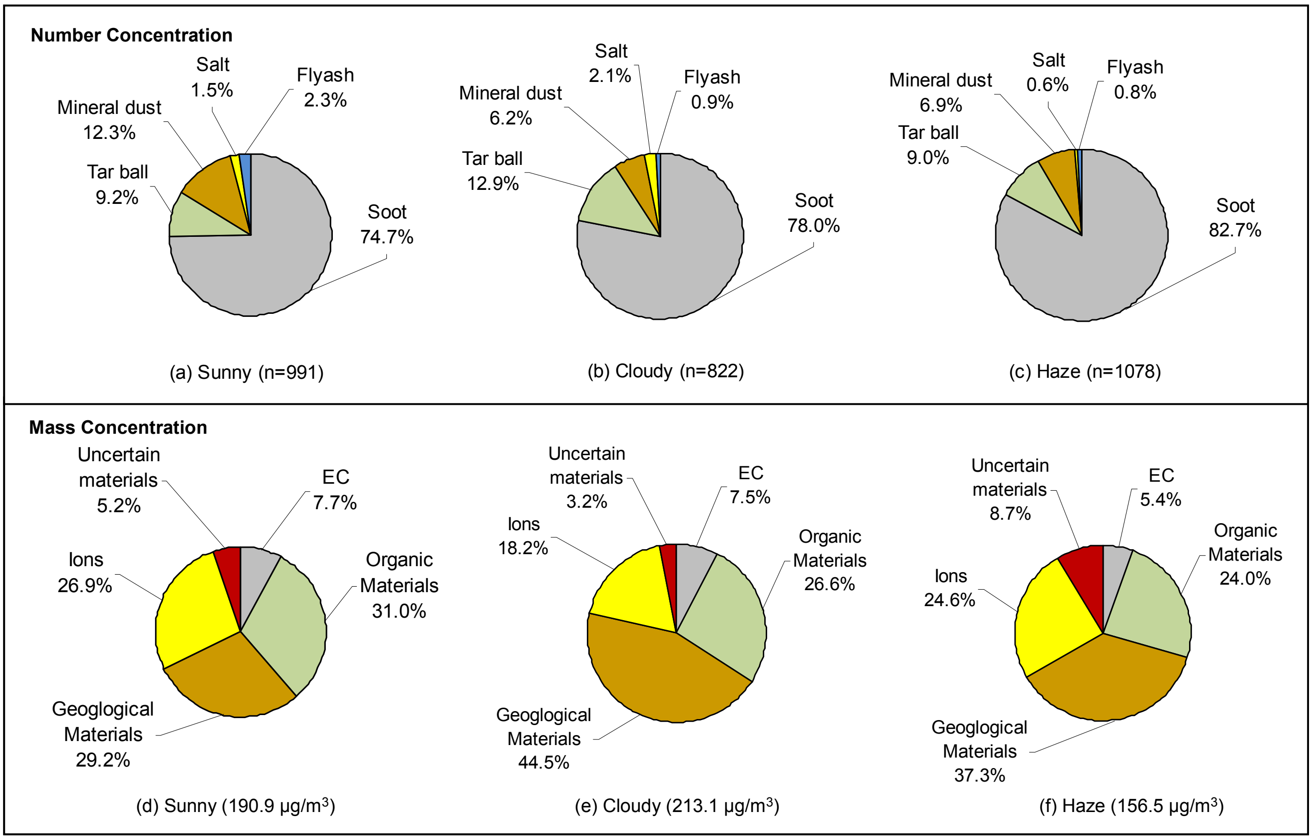

Fig. 5. Particle classification and number concentrations of major constituents determined by individual particle analysis (a, b, and c in upper box) and material balance charts determined by chemical bulk analyses (d, e, and f in lower box) for $PM_{2.5}$ in Xi'an.

to "soot" type according to their morphologies, the relatively lower number concentration of tar ball (9.0–12.9%) in $PM_{2.5}$ in Xi'an was obtained when compared with bulk chemical OM results (24.0–31.0%). As chemical tracer for biomass burning, the mass concentrations of K^+ in this study are lower than those in straw combustion days, but higher than those in normal days in Xi'an (Shen *et al.*, 2009). Therefore, biomass burning was one source but not the main source of winter $PM_{2.5}$ in Xi'an.

Geological Materials

Corresponding to geological material in mass concentration charts determined by bulk analysis, mineral dust and fly ash were classified in number concentration charts according to their elemental composition enriched by Al and Si, and minor Na, Mg, Ca, Mn, and Fe. The mass concentrations of geological materials on the sunny, cloudy, and hazy days were 29.2%, 44.5%, and 37.3%, respectively. The number concentrations of mineral dust and fly ash on the sunny, cloudy, and hazy days were added up to 14.6%, 7.1%, and 7.7%, respectively. Mineral dust, mostly with irregular shape, was composed of silicate, quartz, sulfate, carbonate and aluminosilicate, which could come either from resuspended construction and road dust, or from transport of fugitive dust. Spherical fly ash particles were generally aluminosilicate or silicate glasses from coal combustion, which had a range of compositions similar to clay minerals.

Since element N was excluded in EDX analysis, ammonium and nitrate salts were undetectable with individual particle analysis. Only ammonium sulfate particle could be presumed according to its morphology and EDX spectrum (Hu *et al.*, 2010). In our study, bulk IC analysis provided the mass concentrations of all 8 ions (shown as ions in lower box of Fig. 5), whereas individual particle analysis only identified sulfate and chloride in numbers (illustrated as salts in upper box of Fig. 5).

CONCLUSION

Size-differentiated winter TSP, PM_{10}, $PM_{2.5}$, and PM_1 were analyzed with SEM-EDX to obtain a comprehensive view on particle morphologies and chemical compositions. According to the number percentages of major constituent, carbonaceous particles predominated in all the size range aerosols collected in Xi'an city.

Chemical bulk analysis was also introduced into $PM_{2.5}$ characterization. The inter-comparison of mass and number concentrations of major constituents in $PM_{2.5}$ suggested that bulk and individual particle analytical techniques should be incorporated into detailed atmospheric aerosol characterization.

Soot was always the dominating component (in numbers) in size-differentiated samples. Due to their small size and loose structure, the contribution of soot aggregates to the total $PM_{2.5}$ mass was relatively small. Thus, studies on the basis of bulk analysis techniques may have underestimated the human health risk associated with this component. Since there exists evidence that aerosol adverse health effects are related to particle numbers (Hoek *et al.*, 2002), individual particle analysis could be used to assess the emission from fossil fuel combustion and biomass burning processes.

Aluminosilicate and silica from anthropogenic and natural sources are with distinguished morphologies. Most of them from natural sources are non-spherical, whereas those from anthropogenic sources are normally spherical fly ashes. At present, it is impossible for bulk analytical methods to discriminate between the two sources of alumosilicates and silica. Therefore, aerosol components from crustal source could be overestimated when Si and Al are detectable by elemental analysis and used as tracer for natural sources.

ACKNOWLEDGMENTS

This work was supported in part by the Natural Science Foundation of China (NSFC40925009), projects from Chinese Academy of Sciences (No O929011018 and KZCX2-YW-BR-10) and Ministry of Science and Technology (2009IM030100).

REFERENCES

Anderson, H.R., Bremner, S.A., Atkinson, R.W., Harrison, R.M. and Walters, S. (2001). Particulate Matter and Daily Mortality and Hospital Admissions in the West Midlands Conurbation of the United Kingdom: Associations with Fine and Coarse Particles, Black Smoke and Sulphate. *Occup. Environ. Med.* 58: 504–510.

Avino, P., Casciardi, S., Fanizza, C. and Manigrasso, M. (2011). Deep Investigation of Ultrafine Particles in Urban Air. *Aerosol Air Qual. Res.* 11: 654–663.

Bond, T.C., Streets, D.G., Yarber, K.F., Nelson, S.M., Woo, J.H. and Klimont, Z. (2004). A technology-based Global Inventory of Black and Organic Carbon Emissions from Combustion. *J. Geophys. Res.* 109: D14203, doi: 10.1029/2003JD003697.

Cao, J.J., Lee, S.C., Ho, K.F., Zhang, X.Y., Zou, S.C., Fung, K., Chow, J.C. and Watson, J.G. (2003). Characteristics of Carbonaceous Aerosol in Pearl River Delta Region China during 2001 Winter Period. *Atmos. Environ.* 37: 1451–1460.

Cao, J.J., Wu, F., Chow, J.C., Lee, S.C., Li, Y., Chen, S.W., An, Z.S., Fung, K.K., Watson, J.G., Zhu, C.S. and Liu, S.X. (2005a). Characterization and Source Apportionment of Atmospheric Organic and Elemental Carbon during Fall and Winter of 2003 in Xi'an, China. *Atmos. Chem. Phys.* 5: 3127–3137.

Cao, J.J., Lee, S.C., Zhang, X.Y., Chow, J.C., An, Z.S., Ho, K.F., Watson, J.G., Fung, K., Wang, Y.Q. and Shen, Z.X. (2005b). Characterization of Airborne Carbonate over a Site near Asian Dust Source Regions during Spring 2002 and its Climatic and Environmental Significance. *J. Geophys. Res.* 110: D03203, doi: 10.1029/2004JD005244.

Cao, J.J., Zhang, T., Chow, J.C., Watson, J.G., Wu, F. and Li, H. (2009). Characterization of Atmospheric Ammonia over Xi'an, China. *Aerosol Air Qual. Res.* 9: 277–289.

Cao, J.J., Li, H., Chow, J.C., Watson, J.G., Lee, S.C., Rong, B., Dong, J.G. and Ho, K.F. (2011). Chemical Composition of Indoor and Outdoor Atmospheric Particles at Emperor Qin's Terra-cotta Museum, Xi'an, China. *Aerosol Air Qual. Res.* 11: 70–79.

Chakrabarty, R.K., Moosmüller, H., Garro, M.A., Arnott, W.P., Walker, J., Susott, R.A., Babbitt, R.E., Wold, C.E., Lincoln, E.N. and Hao, W.M. (2006). Emissions from the Laboratory Combustion of Wildland Fuels: Particle Morphology and Size. *J. Geophys. Res.* 111: D07204, doi: 10.1029/2005JD006659.

Cheng, Y.H. and Lin, Y.L. (2010). Measurement of Particle Mass Concentrations and Size Distributions in an Underground Station. *Aerosol Air Qual. Res.* 10: 22–29

Chow, J.C. and Watson, J.G. (1999). In *Elemental Analysis of Airborne Particles*, Vol. 1, Ion Chromatography in Elemental Analysis of Airborne Particles, Landsberger, S. and Creatchman, M. (Eds.), Gordon and Breach Science, Amsterdam, p. 97–137.

Dachs, J. and Eisenreich, S.J. (2000). Adsorption onto Aerosol Soot Carbon Dominates Gas-particle Partitioning of Polycyclic Aromatic Hydrocarbons. *Environ. Sci. Technol.* 34: 3690–3697.

Diapouli, E., Eleftheriadis, K., Karanasiou, A.A., Vratolis, S., Hermansen, O., Colbeck, I. and Lazaridis, M. (2011). Indoor and Outdoor Particle Number and Mass Concentrations in Athens. Sources, Sinks and Variability of Aerosol Parameters. *Aerosol Air Qual. Res.* 11: 632–642.

Edgerton, E.S., Casuccio, G.S., Saylor, R.D., Lersch, T.L., Hartsell, B.E, Jansen, J.J. and Hansen, D.A. (2009). Measurements of OC and EC in Coarse Particulate Matter in the Southeastern United States. *J. Air Waste Manage. Assoc.* 59: 78–90.

Han, Y.M., Cao, J.J., Chow, J.C., Watson, J.G., An, Z.S., Jin, Z., Fung, K. and Liu, S. (2007). Evaluation of the Thermal/Optical Reflectance Method for Discrimination between Char- and Soot-EC. *Chemosphere* 69: 569–574.

Hand, J.L., Malm, W.C., Laskin, A., Day, D., Lee, T., Wang, C., Carrico, C., Carrillo, J., Cowin, J.P., Collett, J. and Iedema, M.J. (2005). Optical, Physical, and Chemical Properties of Tar Balls Observed during the Yosemite Aerosol Characterization Study. *J. Geophys. Res.* 110: D21210, doi: 10.1029/2004JD005728.

Harrison, R.M. and Yin, J. (2000). Particulate Matter in the Atmosphere: Which Particle Properties Are Important for Its Effects on Health? *Sci. Total Environ.* 249: 85–101.

Harrison, R.M., Jones, A.M. and Lawrence, R.G. (2004). Major Component Composition of PM_{10} and $PM_{2.5}$ from Roadside and Urban Background Sites. *Atmos. Environ.* 38: 4531–4538.

Hoek, G., Brunekreef, B., Goldbohm, S., Fischer, P. and van den Brandt, P.A. (2002). Association between Mortality and Indicators of Traffic-related Air Pollution in The Netherlands: A Cohort Study. *Lancet* 360: 1203–1209.

Hu, T., Lee, S., Cao, J., Chow, J.C., Watson, J.G., Ho, K., Ho, W., Rong, B. and and An, Z. (2009). Characterization of Winter Airborne Particles at Emperor Qin's Terra-cotta Museum, China. *Sci. Total Environ.* 407: 5319–5327.

Hu, T., Cao, J., Lee, S., Li, X., Shen, Z., Rong, B., An, Z. (2010). Microanalysis of Dust Deposition inside Emperor Qin's Terra-Cotta Warriors and Horses Museum. *Aerosol Air Qual. Res.* 10: 59–66.

Huang, S.L., Hsu, M.K. and Chan, C.C. (2003). Effects of Submicrometer Particle Compositions on Cytokine Production and Lipid Peroxidation of Human Bronchial Epithelial Cells. *Environ. Health Perspect.* 111: 478–482.

Hussein, T., Al-Ruz, R.A., Petäjä, T., Junninen, H., Arafah, D.E., Hämeri, K. and Kulmala, M. (2011). Local Air Pollution versus Short–range Transported Dust Episodes: A Comparative Study for Submicron Particle Number Concentration. *Aerosol Air Qual. Res.* 11: 109–119.

Laden, F., Neas, L.M., Dockery, D.W. and Schwartz, J. (2000). Association of Fine Particulate Matter from Different Sources with Daily Mortality in Six US Cities. *Environ. Health Perspect.* 108: 941–947.

Laskin, A., Wietsma, T.W., Krueger, B.J. and Grassian, V.H. (2005). Heterogeneous Chemistry of Individual Mineral Dust Particles with Nitric Acid: A Combined CCSEM/EDX, ESEM, and ICP-MS Study. *J. Geophys. Res.* 110: D10208, doi: 10.1029/2004JD005206.

Li, J., Pósfai, M., Hobbs, P.V. and Buseck, P.R. (2003). Individual Aerosol Particles from Biomass Burning in Southern Africa: 2, Compositions and Aging of Inorganic Particles. *J. Geophys. Res.* 108: 8484, doi: 10.1029/2002 JD002310.

O'Dowd, C.D., Facchini, M.C., Cavalli, F., Ceburnis, D., Mircea, M., Decesari, S., Fuzzi, S., Yoon, Y.J. and Putaud, J.P. (2004). Biogenically Driven Organic Contribution to Marine Aerosol. *Nature* 431: 676–680.

Pósfai, M., Anderson, J.R. and Buseck, P.R. (1999). Soot and Sulfate Aerosol Particles in the Remote Marine Troposphere. *J. Geophys. Res.* 104: 21685–21693.

Pósfai, M., Simonics, R., Li, J., Hobbs, P.V. and Buseck, P.R. (2003). Individual Aerosol Particles from Biomass Burning in Southern Africa: 1. Compositions and Size Distributions of Carbonaceous Particles. *J. Geophys. Res.* 108: 8483. doi: 10.1029/2002JD002291.

Pósfai, M., Gelencsér, A., Simonics, R., Arató, K., Li, J., Hobbs, P.V. and Buseck, P.R. (2004). Atmospheric Tar Balls: Particles from Biomass and Biofuel Burning, *J. Geophys. Res.* 109: D06213, doi: 10.1029/2003JD004169.

Seinfeld, J.H. and Pankow, J.F. (2003). Organic Atmospheric Particulate Material. *Annu. Rev. Phys. Chem.* 54: 121–140.

Shen, Z.X., Arimoto, R., Okuda, T., Cao, J.J., Zhang, R.J., Li, X.X., Du, N., Nakao, S. and Tanaka, S. (2008). Seasonal Variations and Evidence for the Effectiveness of Pollution Controls on Water-soluble Inorganic Species in TSP and $PM_{2.5}$ from Xi'an, China. *J. Air Waste Manage. Assoc.* 58: 1560–1570.

Shen, Z.X., Cao, J.J., Arimoto, R., Han, Z.W., Zhang, R.J., Han, Y.M., Liu, S.X., Okuda, T., Nakao, S. and Tanaka, S. (2009). Ionic Composition of TSP and $PM_{2.5}$ during Dust Storms and Air Pollution Episodes at Xi'an, China. *Atmos. Environ*. 43: 2911–2918.

Shen, Z.X., Han, Y.M., Cao, J.J., Tian, J., Zhu, C.S., Liu, S.X., liu, P.P. and Wang, Y.Q. (2010). Characteristics of Traffic-related Emissions: A Case Study in Roadside Ambient Air over Xi'an, China. *Aerosol Air Qual. Res.* 10: 292–300.

Shen, Z.X., Cao, J.J., Liu, S.X., Zhu, C.S., Wang, X., Zhang, T., Xu, H.M. and Hu, T.F. (2011). Chemical Composition of PM_{10} and $PM_{2.5}$ Collected at Ground Level and 100 Meters during a Strong Winter-Time Pollution Episode in Xi'an, China. *J. Air Waste Manage. Assoc.* 61: 1150–1159.

Solomon, P.A., Fall, T., Salmon, L., Cass, G.R., Gray, H.A. and Davidson, A. (1989). Chemical Characteristics of PM_{10} Aerosols Collected in the Los Angeles Area. *J. Air Pollut. Contr. Assoc.* 39: 154–163.

Sun, J. and Ariya, P.A. (2006). Atmospheric Organic and Bio-aerosols as Cloud Condensation Nuclei (CCN): A Review. *Atmos. Environ.* 40: 795–820.

Tai, A.P.K.; Mickley, L.J. and Jacob, D.J. (2010). Correlations between Fine Particulate Matter ($PM_{2.5}$) and Meteorological Variables in the United States: Implications for the Sensitivity of $PM_{2.5}$ to Climate Changes. *Atmos. Environ.* 44: 3976–3984.

Taylor, S.R. and Mclennan, S.M. (1985). *The Continental Crust: Its Composition and Evolution*, Oxford. Blackwell p. 315.

Tivanski, A.V., Hopkins, R.J., Tyliszczak, T. and Gilles, M.K. (2007). Oxygenated Interface on Biomass Burn Tar Balls Determined by Single Particle Scanning Transmission X-ray Microscopy. *J. Phys. Chem. A* 111: 5448–5458.

Turpin, B.J. and Lim, H.J. (2001). Species contributions to $PM_{2.5}$ Mass Concentrations: Revisiting common Assumptions for Estimating Organic Mass. *Aerosol Sci. Technol.* 35: 602–610.

U.S. Environmental Protection Agency. (2004). Air Quality Criteria for Particulate Matter. Research Triangle Park, NC: National Center for Environmental Assessment-RTP Office, Report No. EPA/600/P-99/OOa2F.

Watson, J.G., Chow, J.C. and Houck, J.E. (2001). $PM_{2.5}$ Chemical Source Profiles for Vehicle Exhaust, Vegetative Burning, Geological Material, and Coal Burning in Northwestern Colorado during 1995. *Chemosphere* 43: 1141–1151.

Watson, J.G. (2002). Visibility: Science and Regulation. *J. Air Waste Manage. Assoc.* 52: 628–713.

Watson, J.G., Chow, J.C. and Chen, L.-W.A. (2005). Summary of Organic and Elemental Carbon/Black Carbon Analysis Methods and Intercomparisons. *Aerosol Air Qual. Res.* 5: 65–102.

Xu, H.M., Cao, J.J., Ho, K.F., Ding, H., Han, Y.M., Wang, G.H., Chow, J.C., Watson, J.G., Khol, S.D., Qiang, J. and Li, W.T. (2011). Lead Concentrations in Fine Particulate Matter after the Phasing out of Leaded Gasoline in Xi'an, China. *Atmos. Environ*. 46: 217–224.

Yin, J. and Harrison, R.M. (2008). Pragmatic Mass Closure Study for $PM_{1.0}$, $PM_{2.5}$ and PM_{10} at Roadside, Urban Background and Rural Sites. *Atmos. Environ.* 42: 980–988.

Zhang, D., Iwasaka, Y. and Shi, G. (2001). Soot Particles and their Impacts on the Mass Cycle in the Tibetan Atmosphere. *Atmos. Environ.* 35: 5883–5894.

Zhang, R., Arimoto, R., An, J., Yabuki, S. and Sun J. (2005). Ground Observations of a Strong Dust Storm in Beijing in March 2002, *J. Geophys. Res.* 110: D18S06, doi: 10.1029/2004JD004589.

Zhang, R.J., Shen, Z.X., Zou, H., Wang, W., Han, Y.M. and Zhou, J. (2008). Study of Elemental Mass Size Distributions of Aerosol in Lijiang, a Background Site in Southwest China. *Aerosol Air Qual. Res.* 8: 339–347.

Zhang, X.Y., Cao, J.J., Li, L.M., Arimoto, R., Cheng, Y., Huebert, B. and Wang, D. (2002). Characterization of Atmospheric Aerosol over Xi'an in the South Margin of the Loess Plateau, China. *Atmos. Environ.* 36: 4189–4199.

Zhang, X.Y., Gong, S.L., Arimoto, R., Shen, Z.X., Mei, F.M., Wang D. and Cheng Y. (2003). Characterization and Temporal Variation of Asian Dust Aerosol from a Site in the Northern Chinese Deserts. *J. Atmos. Chem.* 44: 241–257.

Zhu, C.S., Cao, J.J., Tsai, C.J., Shen, Z.X., Ho, K.F. and Liu, S.X. (2010). The Indoor and Outdoor Carbonaceous Pollution during Winter and Summer in Rural Areas of Shaanxi, China. *Aerosol Air Qual. Res.* 10: 550–558.

Received for review, January 15, 2012
Accepted, March 29, 2012